Human Molecular Genetics, 2001, Vol. 10, No. 19 **2069–2077**

Gestational, pathologic and biochemical differences between very long-chain acyl-CoA dehydrogenase deficiency and long-chain acyl-CoA dehydrogenase deficiency in the mouse

Keith B. Cox, Doug A. Hamm, David S. Millington[1], Dietrich Matern[2], Jerry Vockley[3], Piero Rinaldo[2], Carl A. Pinkert, William J. Rhead[4], J. Russell Lindsey and Philip A. Wood*

Department of Genomics and Pathobiology, 1670 University Boulevard, University of Alabama at Birmingham, Birmingham, AL 35294-0019, USA, [1]Mass Spectrometry Facility, Duke University, Research Triangle Park, NC 27709, USA, [2]Department of Laboratory Medicine and Pathology and [3]Department of Medical Genetics, Mayo Clinic, Rochester, MN 55905, USA and [4]Department of Pediatrics, University of Iowa, Iowa City, IA 52242, USA

Received April 17, 2001; Revised and Accepted July 13, 2001

Although many patients have been found to have very long-chain acyl-CoA dehydrogenase (VLCAD) deficiency, none have been documented with long-chain acyl-CoA dehydrogenase (LCAD) deficiency. In order to understand the metabolic pathogenesis of long-chain fatty acid oxidation disorders, we generated mice with VLCAD deficiency (VLCAD$^{-/-}$) and compared their pathologic and biochemical phenotypes of mice with LCAD deficiency (LCAD$^{-/-}$) and wild-type mice. VLCAD$^{-/-}$ mice had milder fatty change in liver and heart. Dehydrogenation of various acyl-CoA substrates by liver, heart and skeletal muscle mitochondria differed among the three genotypes. The results for liver were most informative as VLCAD$^{-/-}$ mice had a reduction in activity toward palmitoyl-CoA and oleoyl-CoA (58 and 64% of wild-type, respectively), whereas LCAD$^{-/-}$ mice showed a more profoundly reduced activity toward these substrates (35 and 32% of wild-type, respectively), with a significant reduction of activity toward the branched chain substrate 2,6-dimethylheptanoyl-CoA. C_{16} and C_{18} acylcarnitines were elevated in bile, blood and serum of fasted VLCAD$^{-/-}$ mice, whereas abnormally elevated C_{12} and C_{14} acylcarnitines were prominent in LCAD$^{-/-}$ mice. Progeny with the combined LCAD$^{+/+}$//VLCAD$^{+/-}$ genotype were over-represented in offspring from sires and dams heterozygous for both LCAD and VLCAD mutations. In contrast, no live mice with a compound LCAD$^{-/-}$//VLCAD$^{-/-}$ genotype were detected.

INTRODUCTION

Inborn errors of mitochondrial long-chain fatty acid oxidation (FAO) are emerging as an important cause of Reye syndrome-like metabolic crisis with hypoketotic-hypoglycemia, cardiac arrhythmia and sudden unexpected death (1). Other clinical disease features include cardiac hypertrophy, exertional rhabdomyolysis and liver disease (1). Although very long-chain acyl-CoA dehydrogenase (VLCAD) deficiency in human patients is well characterized (2), no patient with long-chain acyl-CoA dehydrogenase (LCAD) deficiency has been identified (3,4). The severity of disease presentation in disorders of long-chain FAO can be correlated with the specific enzyme affected and the degree of detectable residual enzyme activity *in vitro* (3,5,6). For example, defects that block either long-chain fatty acid (LCFA) transport into the mitochondria or entrance of LCFA acyl-CoAs into the β-oxidation spiral for mitochondrial fatty acid metabolism result in more severe disease. Additionally, the presence of residual enzyme activity results in a milder or even different clinical phenotype. Fatal metabolic crises or fatal arrhythmias are most often seen in neonates or infants with essentially no carnitine palmitoyltransferase II activity (<5%). This contrasts with the exertional rhabdomyolysis seen in adults with some residual activity of carnitine palmitoyltransferase II activity (15–20% of normal activity) (7).

Children with mutations resulting in complete or nearly complete loss of very long-chain acyl-coenzyme A dehydrogenase activity (VLCAD, enzyme; *Acadvl*, mouse gene; *ACADVL*, human gene) may present with hypertrophic cardiomyopathy, hypoketotic-hypoglycemia or sudden death (3). VLCAD functions as a homodimeric protein associated with the inner mitochondrial membrane and catalyzes the initial step of the mitochondrial β-oxidation spiral for LCFA (C_{16} or greater) following the translocation of LCFA acyl-CoA into the mitochondrial matrix (8). Because VLCAD initiates β-oxidation of the most commonly utilized fatty acids, palmitate (C_{16}) and oleate ($C_{18:1}$), it is not surprising that VLCAD deficiency significantly impairs ability to oxidize fatty acids when needed, as during a period of fasting. Until the discovery of VLCAD in the early 1990s, patients diagnosed with deficiencies in VLCAD were considered to have a defect in long-chain acyl-coenzyme A dehydrogenase activity (4) (LCAD, enzyme; *Acadl*, mouse gene; *ACADL*, human gene). LCAD is a

*To whom correspondence should be addressed. Tel: +1 205 934 1303; Fax: +1 205 975 4418; Email: paw@uab.edu

homotetrameric protein of the mitochondrial matrix with similar catalytic activity to VLCAD but with a shorter carbon chain length specificity range, C_{12}–C_{16} (9). Following the discovery of VLCAD, several independent mutant alleles were found to explain VLCAD deficiency (3,10–14). At present, no patients with disease-causing mutations in *ACADL* have been identified. This could arise from either gestational loss due to LCAD deficiency as seen in the mouse model (15), a failure to recognize LCAD deficiency because the phenotype differs so greatly from other inborn errors of fatty acid metabolism, or absence of disease resulting from LCAD deficiency in humans. Gene targeting has been used to ablate LCAD activity in mice (15). LCAD-deficient mice share many of the clinical and metabolic features of patients with VLCAD deficiency (15). To test the hypothesis that the phenotype of VLCAD-deficient mice would mimic the clinical disease seen in VLCAD-deficient patients, we generated mice with ablated VLCAD activity. We then compared the biochemical and pathologic phenotypes of LCAD-deficient mice and VLCAD-deficient mice. We compared these two mouse models with inborn errors of mitochondrial LCFA catabolism to better understand how deficiencies in distinct but closely related enzymes can influence disease severity and progression. These studies should help in better defining the metabolic pathogenesis and diagnostic criteria for investigation and treatment of children with these potentially fatal inborn errors.

RESULTS

Gene targeting for development of VLCAD-deficient mice

Mice with VLCAD deficiency (VLCAD$^{-/-}$ mice) were generated using standard embryonic stem cell techniques as described previously (15). The vector was designed so that the desired recombination event in embryonic stem cells would yield the replacement of exons 7–19 with the selectable neomycin resistance gene (Fig. 1). The designed recombination event resulted in the replacement of exons 7–19 and the first 33 nucleotides of exon 20 with the *neo* gene. Figure 2A demonstrates the *Acadvl* deletion mutation by Southern blot analysis. VLCAD$^{-/-}$ mice produced no detectable VLCAD protein as shown by western blot analysis of isolated mitochondrial proteins from liver (Fig. 2B).

LCAD-deficient mice show reduced litter size

Despite the hybrid vigor expected of breeding pairs with combination 129, B6 genetic backgrounds, LCAD$^{-/-}$ × LCAD$^{-/-}$ breeding pairs produced only 6.7 weaned pups per litter (n = 12) compared with the 8.6 pups per litter observed in VLCAD$^{-/-}$ × VLCAD$^{-/-}$ (n = 7) and 8.5 weaned pups per litter observed in wild-type × wild-type breeding pairs (n = 11). The LCAD$^{-/-}$ breeding pairs produced a significantly lower number of pups ($P < 0.05$) compared with the VLCAD$^{-/-}$ or wild-type matings. The smaller litter sizes of LCAD$^{-/-}$ breeders were expected given our previous observation of under-representation of LCAD$^{-/-}$ and +/– progeny from LCAD$^{+/-}$ × LCAD$^{+/-}$ breeding pairs (15).

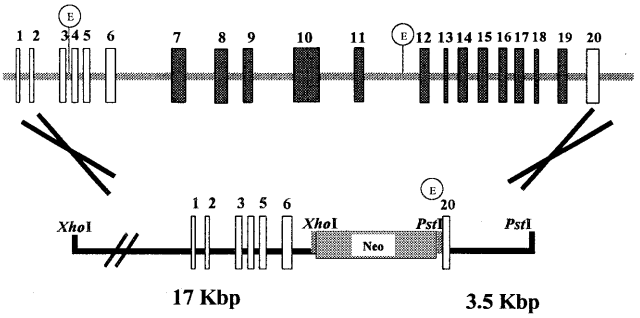

Figure 1. The *Acadvl* targeting vector was constructed from a 17 kb *Xho*I fragment and a 2 kb *Pst*I fragment that flanked the selectable bacterial *neo* gene.

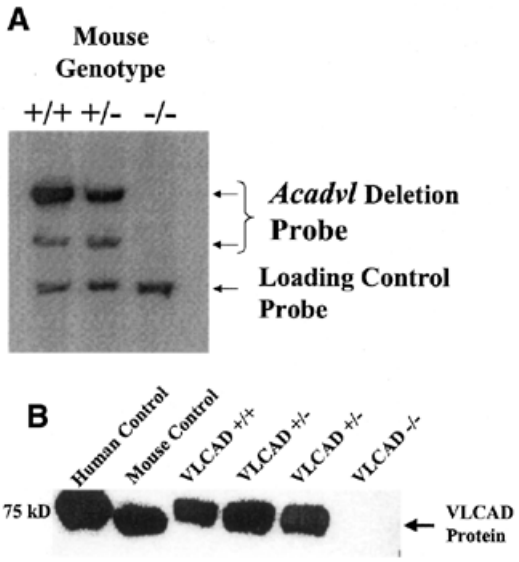

Figure 2. (**A**) Southern blot analysis of wild-type, VLCAD$^{+/-}$ and VLCAD$^{-/-}$ mice. A cDNA probe that spans exons in the deleted region of *Acadvl* was used. The probe hybridizes the *Eco*RI fragments present in the wild-type (+/+) and VLCAD$^{+/-}$ mice but not to DNA isolated from the VLCAD$^{-/-}$ mice, demonstrating that the recombination event resulted in the desired recombination event. (**B**) Western blot analysis of liver isolated mitochondria from wild-type, VLCAD$^{+/-}$ and VLCAD$^{-/-}$ mice probed with rabbit anti-VLCAD antibody. No VLCAD protein was detectable in the mitochondria isolated from VLCAD$^{-/-}$ mice.

Fatty change in liver and heart in LCAD$^{-/-}$ and VLCAD$^{-/-}$ mice in response to fasting

The acute metabolic decompensation in children with inborn errors of FAO is often precipitated by fasting. We fasted LCAD$^{-/-}$ and VLCAD$^{-/-}$ mice and observed that fasting of VLCAD$^{-/-}$ mice was sufficient to produce the histopathologic phenotype, although much milder, but similar to that seen in LCAD$^{-/-}$ mice (15).

Frozen liver sections stained with Oil-Red-O demonstrated the pattern of severity in the metabolic disruption resulting from fasting (Fig. 3). Fasted wild-type mice accumulated only very small triglyceride droplets in the hepatocyte cytoplasm, which were uniformly distributed throughout the

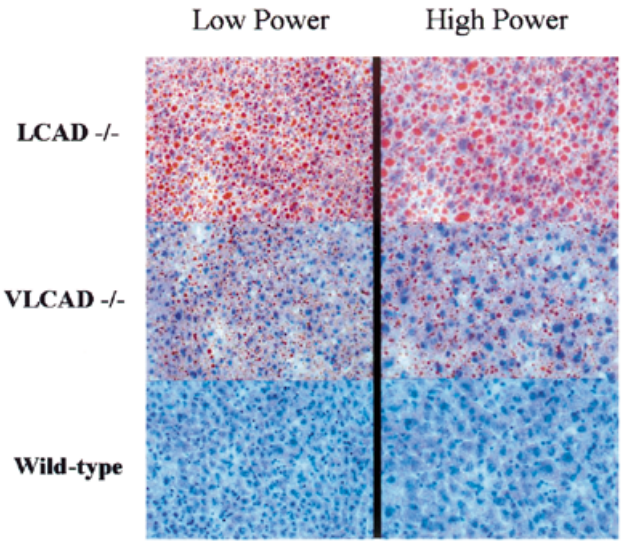

Figure 3. Fasting induced hepatosteatosis in LCAD$^{-/-}$ and VLCAD$^{-/-}$ mice (females, 7–14 weeks old, fasted 24 h). The left column of panels shows low power photomicrographs of Oil-Red-O stained frozen liver sections from LCAD$^{-/-}$, VLCAD$^{-/-}$ and wild-type mice counterstained with eosin. Triglycerides stained magenta against the blue eosin background. Note the large, evenly distributed, positively staining fat droplets in the LCAD$^{-/-}$ panel compared with the patchy distribution of smaller droplets in the VLCAD$^{-/-}$ panel and the small evenly distributed droplets in the wild-type panel. The right column of photomicrographs display higher power images that show the large fat droplets in the LCAD$^{-/-}$ panel compared with the mixed medium and small droplets in the VLCAD$^{-/-}$ mice and the small droplets in wild-type mice.

hepatic lobules. In contrast, livers of VLCAD$^{-/-}$ mice showed mild steatosis with droplets of varying sizes in many hepatocytes. Using low-power magnification the distribution of more prominently stained cells was notably uneven within and among lobules resulting in a patchy staining pattern. In contrast, LCAD$^{-/-}$ mice showed blatant, severe hepatosteatosis with a preponderance of large, uniformly distributed droplets throughout their livers. Similar studies of hearts from the VLCAD mutants showed a mild, diffuse fatty change (not shown) in contrast to profound fatty change in hearts from LCAD mutants as reported previously (15). There were no other histopathologic lesions found in the VLCAD mutants.

Long-chain acyl-CoA dehydrogenation in LCAD- and VLCAD-deficient mice

We hypothesized that substrate overlap between LCAD and VLCAD in mice could explain the overall attenuation in phenotype severity of mice with VLCAD deficiency compared with humans. To test this question VLCAD and LCAD enzyme activities were measured by electron transport flavoprotein (ETF) reduction for different straight and branch-chain fatty acids in liver, and in cardiac and skeletal muscle (Table 1).

Enzyme activity toward each substrate was about 10-fold higher in cardiac than skeletal muscle or liver (Table 1). Although enzyme activity toward octanoyl-CoA was similar in all genotypes, LCAD$^{-/-}$ mice showed a modest loss of activity in all three tissues. Surprisingly, no differences in activity toward palmitoyl-CoA were seen between VLCAD$^{-/-}$ mice and wild-type mice in heart tissue, and LCAD activity appeared to account for much of the activity toward oleoyl-CoA. Only LCAD$^{-/-}$ mice demonstrated a profound decrease in activity toward the branched-chain substrate, 2,6-dimethylheptanoyl-CoA, a substrate specific for LCAD *in vitro* (16).

Acylcarnitine profile analyses in LCAD- and VLCAD-deficient mice

Detection of abnormal concentrations of acylcarnitines in body fluids using mass spectrometry has become a common tool for the biochemical diagnosis of inborn errors of metabolism in human beings. We have applied this analysis to samples collected from our mouse models. Saturated and unsaturated acylcarnitine esters were detected in serum, bile and whole blood spotted onto filter paper, and frozen skeletal muscle and heart tissues from fasted mutant and wild-type mice.

Serum acylcarnitine analysis clearly distinguished LCAD deficiency from VLCAD deficiency (Fig. 4A). Bile acylcarnitine analysis most clearly and vividly reveals the trends in abnormal metabolite formation in VLCAD$^{-/-}$ and LCAD$^{-/-}$ mice (Fig. 4B). The acylcarnitine concentrations are ~50–100-fold higher in bile than in serum or whole blood. In the case of LCAD$^{-/-}$ mice, C_{10}, C_{12} and C_{14} acylcarnitine esters were significantly elevated ($P < 0.05$) with prominent increases in C_{14} acylcarnitine esters. In contrast, abnormal acylcarnitine species seen in VLCAD$^{-/-}$ mice were predominantly C_{16} and C_{18} acylcarnitines, with only a modest rise in C_{14} species. The concentration of total acylcarnitine metabolites in LCAD$^{-/-}$ mice was higher than that seen in VLCAD$^{-/-}$ mice (223 versus 177 μmol/l). Furthermore, the increases in the concentrations of abnormal acylcarnitine metabolites relative to wild-type values were proportionally higher in LCAD$^{-/-}$ mice than in VLCAD$^{-/-}$ mice (5–55-fold for LCAD$^{-/-}$ mice versus 4–7-fold in VLCAD$^{-/-}$ mice).

Blood spot acylcarnitine profiles of mutant and wild-type mice are depicted in Figure 5. $C_{14:2}$ and $C_{14:1}$ acylcarnitine esters were the most prominently elevated acylcarnitines of LCAD$^{-/-}$ mice, whereas C_{16} and $C_{18:1}$ acylcarnitines were the most abundant in VLCAD$^{-/-}$ mice. Differences between bile and blood spot profiles of VLCAD$^{-/-}$ mice included the relatively greater abundance of C_{16} acylcarnitine esters and the relative paucity of C_{18} acylcarnitine esters in blood. As in bile, relative to wild-type levels the C_{14} acylcarnitine ester levels in LCAD$^{-/-}$ mice were proportionally higher than C_{16} and C_{18} acylcarnitine levels in VLCAD$^{-/-}$ mice. As expected, serum acylcarnitine profiles closely resembled blood spot profiles except that C_{16} acylcarnitine concentrations are approximately half of those seen in blood for all genotypes (Fig. 4A). Skeletal and cardiac tissue acylcarnitine profiles proved less informative than those of body fluids. No significant differences were seen in any acylcarnitine metabolite levels in cardiac muscle. In skeletal muscle, the only significantly elevated acylcarnitines were C_{16} and C_{18} acylcarnitine esters in VLCAD$^{-/-}$ mice (data not shown), also observed to be elevated in bile and blood.

Serum and liver tissue fatty acid profiles

Free fatty acid (FFA) profiles were obtained for serum and liver. Serum fatty acids $C_{14:2}$ and $C_{14:1}$ were significantly elevated in LCAD$^{-/-}$ mice with respect to wild-type and VLCAD$^{-/-}$ mice (data not shown). There were no significant

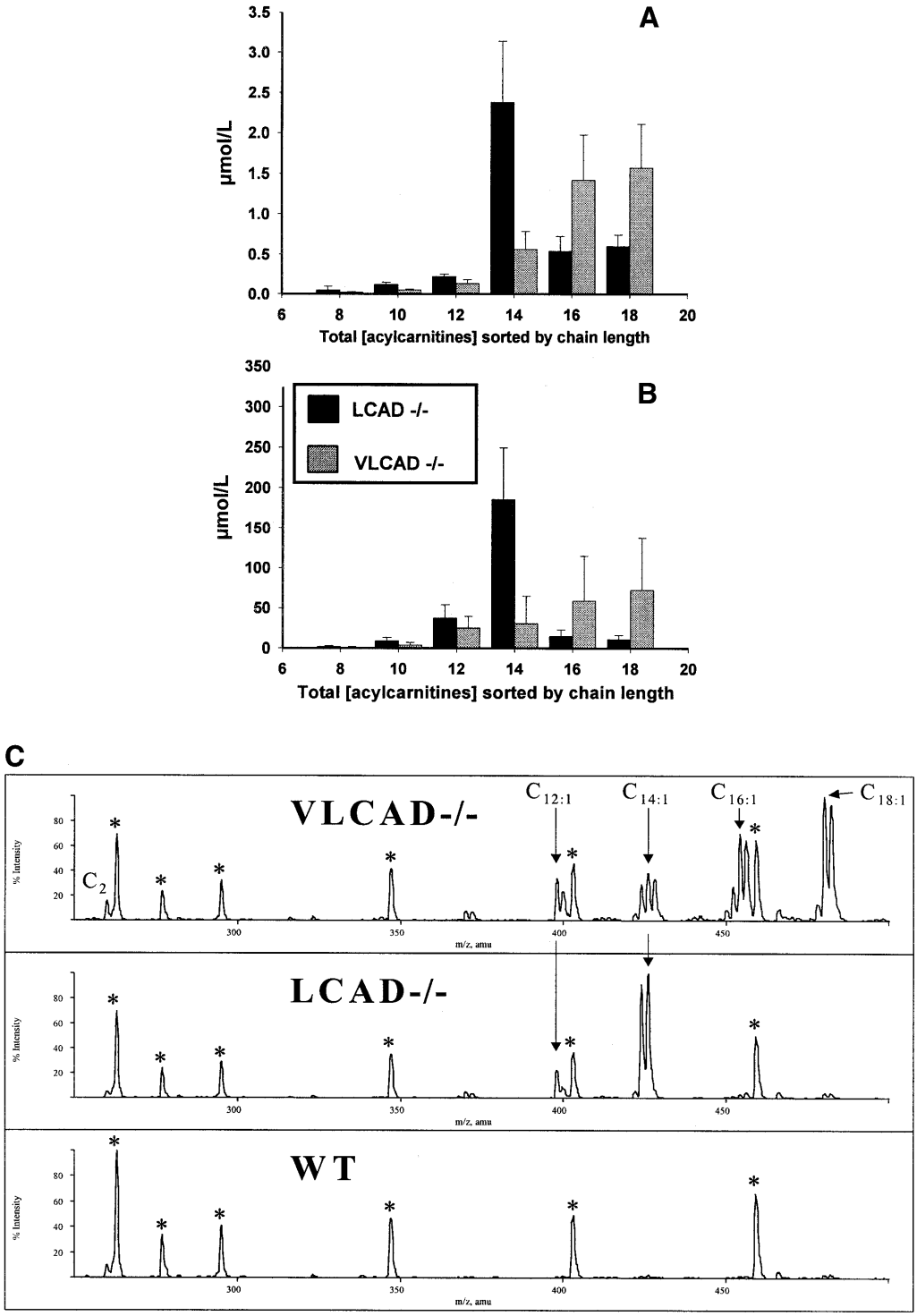

Figure 4. Serum and bile acylcarnitine analysis of LCAD$^{-/-}$ and VLCAD$^{-/-}$ mice (males, 7–14 weeks old, fasted 24 h). (**A**) Serum. (**B**) Bile. Pattern of accumulation of acylcarnitine species in LCAD$^{-/-}$ (solid bars, $n = 4$) and VLCAD$^{-/-}$ (gray bars, $n = 4$) mice expressed at total concentration of all acylcarnitine species of a given chain length. Each bar corresponds to the average value calculated from the analysis of four specimens of each genotype. The error bars indicate standard deviations. (**C**) Comparative chromatographic display of distinct peaks of bile acylcarnitines. Acylcarnitines (butylesters, precursor 85 m/z scan) in bile from a VLCAD$^{-/-}$ (top), LCAD$^{-/-}$ (middle) and wild-type (bottom) mouse. Asterisks denote the deuterated internal standards for acetylcarnitine (C_2), propionylcarnitine (C_3), butyrylcarnitine (C_4), octanoylcarnitine (C_8), dodecanoylcarnitine (C_{12}) and palmitoylcarnitine (C_{16}) (from left to right).

differences in serum FFA concentrations found in the VLCAD$^{-/-}$ mice compared with wild-type controls. Furthermore, only LCAD$^{-/-}$ mice showed significant accumulations of liver fatty acids (Fig. 6). Myristate (C_{14}) was the abnormal fatty acid

Table 1. ETF reduction analysis of mitochondrial acyl-CoA dehydrogenase activity (mU/mg protein) toward a range of acyl-CoA substrates

Substrate	Liver			Heart			Skeletal muscle		
	Wild-type	VLCAD$^{-/-}$	LCAD$^{-/-}$	Wild-type	VLCAD$^{-/-}$	LCAD$^{-/-}$	Wild-type	VLCAD$^{-/-}$	LCAD$^{-/-}$
Octanoyl-CoA	44.0 ± 0.4	42.5 ± 1.4	33.1 ± 2.7	182 ± 14	187 ± 3	169 ± 7	12.0 ± 0.03	17.0 ± 0.7	16.0 ± 0.3
Palmitoyl-CoA	19.6 ± 2.1	11.3 ± 0.3	6.9 ± 0.5	68 ± 10	69 ± 3	29 ± 3	10.0 ± 0.1	7.0 ± 0.4	7.0 ± 0.2
2,6-Dimethyl heptanoyl-CoA	12.4 ± 1.0	10.3 ± 0.3	1.5 ± 0.4	66 ± 5	66 ± 3	0	7.0 ± 1.2	7.0 ± 1.2	0
Oleoyl-CoA	14.3 ± 0.3	9.2 ± 0.7	4.6 ± 0.6	n.d.	n.d.	n.d.	n.d.	n.d.	n.d.

n.d., not determined. 0 indicates no detectable activity.

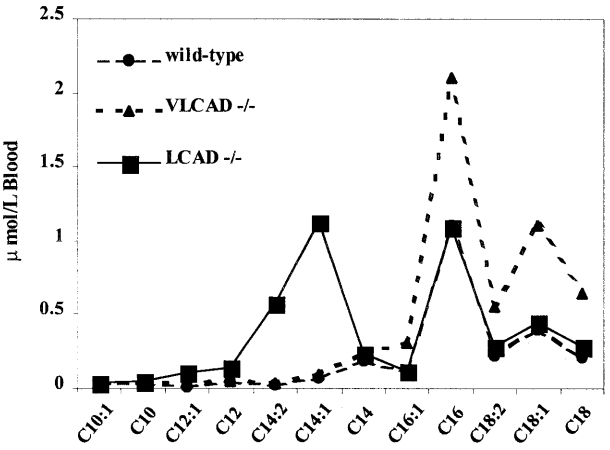

Figure 5. Blood spot acylcarnitine profiles from LCAD$^{-/-}$ (n = 3), VLCAD$^{-/-}$ (n = 4) and wild-type (n = 4) mice (males, 7–14 weeks old, fasted 24 h) closely resemble those obtained from bile and serum. LCAD$^{-/-}$ mice show significant elevations in C_{12}, $C_{12:1}$, $C_{14:2}$ and $C_{14:1}$ acylcarnitine species while VLCAD$^{-/-}$ mice show significant increases in $C_{16:1}$, $C_{16:2}$, C_{16}, $C_{18:1}$ and $C_{18:2}$ acylcarnitine species ($P < 0.05$, one way ANOVA).

Table 2. Genotype distribution of progeny from LCAD$^{+/-}$, VLCAD$^{+/-}$ breeding pairs

Genotype	Observed number	Expected number	χ^2 value
LLVV	7	4.81	1.00
LLVv	20	9.63	11.17
Llvv	8	4.81	2.12
LlVV	5	9.63	2.23
LlVv	17	19.25	0.26
Llvv	8	9.63	0.28
llVV	6	4.81	0.29
llVv	6	4.81	1.37
llvv	0	4.81	4.81
	Total χ^2 value		23.52 ($P < 0.005$)

Wild-type alleles signified by upper case letters and targeted mutant alleles by lower case letters. L, wild-type LCAD; V, wild-type VLCAD; l, mutant LCAD; v, mutant VLCAD.

with the highest absolute elevation, but $C_{14:1}$ showed the largest proportionate increase with respect to wild-type levels.

Urine organic acids

Evaluation of the urine for abnormal dicarboxylic acid metabolites resulted in the detection of significantly elevated suberic acid ($C_{8:0}$) (108 ± 36 mmol/mol creatinine) and octenedioic acid ($C_{8:1}$) (127 ± 96 mmol/mol creatinine) in fasted LCAD$^{-/-}$ mice (n = 4) compared with suberic acid ($C_{8:0}$) (17 ± 17 mmol/mol creatinine) and octenedioic acid ($C_{8:1}$) (17 ± 4.8 mmol/mol creatinine) in wild-type mice (n = 4) ($P < 0.05$). Fasting of VLCAD$^{-/-}$ mice (n = 5) for 24–28 h evoked no significant accumulations of urine dicarboxylic acids compared with wild-type mice. In contrast, there is an absence of abnormal urine metabolites in both LCAD$^{-/-}$ and VLCAD$^{-/-}$ mice when fed and unstressed (data not shown).

Genotype distribution in progeny of LCAD$^{+/-}$//VLCAD$^{+/-}$ breeding pairs

The varying disease severity and biochemical phenotypes arising from LCAD and VLCAD deficiencies suggest that specific metabolic effects resulting from the respective deficiencies may contribute to disease severity in an independent, additive manner. To test this hypothesis, we attempted to generate mice in which both LCAD and VLCAD activities were ablated. Breeding pairs were set up using mice that were heterozygous at both loci. A total of 77 weaned progeny were genotyped. Table 2 shows the observed progeny genotype distribution. Expected numbers were calculated based on a Mendelian distribution pattern of 77 pups. The observed genotype distribution significantly differed from the expected distribution ($P < 0.005$). Two groups, LCAD$^{-/-}$// VLCAD$^{-/-}$ and LCAD$^{+/+}$//VLCAD$^{+/-}$, were striking in their disproportionate representation. No LCAD$^{-/-}$//VLCAD$^{-/-}$ pups were observed. Subsequent genotype examination of partially cannibalized pups from two LCAD$^{-/-}$//VLCAD$^{+/-}$ × LCAD$^{-/-}$// VLCAD$^{+/-}$ breeding pairs resulted in the detection of five LCAD$^{-/-}$//VLCAD$^{-/-}$ pups indicating that loss of these progeny occurred as late as the periparturient period. Curiously, LCAD$^{+/+}$//VLCAD$^{+/-}$ mice were over-represented. This suggests that a competitive advantage existed for progeny heterozygous for VLCAD deficiency but only when both wild-type LCAD alleles were present. A similar trend was noted in the progeny of VLCAD$^{+/-}$ × VLCAD$^{+/-}$ breeding pairs (data not shown).

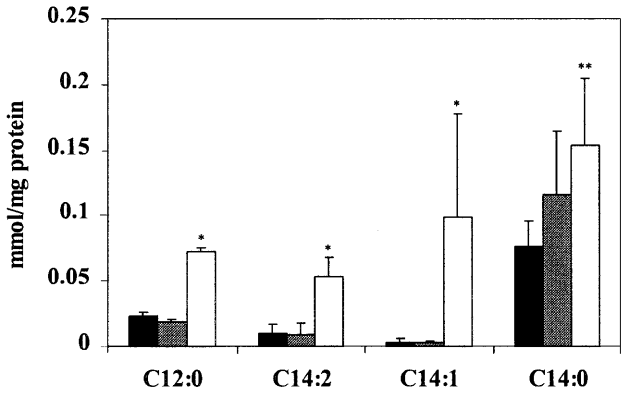

Figure 6. Liver FFA levels were measured in LCAD$^{-/-}$ (n = 5), VLCAD$^{-/-}$ (n = 4) and wild-type (n = 5) mice (males, 7–14 weeks old, fasted 24 h). LCAD$^{-/-}$ mice showed significant increases versus VLCAD$^{-/-}$ and wild-type mice in C_{12}, $C_{14:1}$ and $C_{14:2}$ FFA levels (*$P < 0.05$, one way ANOVA), but $C_{14:0}$ levels in LCAD$^{-/-}$ mice were significantly elevated only with respect to wild-type mice (**$P < 0.05$, one way ANOVA). The error bars indicate standard deviations. Although a full spectrum of fatty acids (C_8–C_{26}) was measured, only those with significant differences were displayed. Black bars, wild-type; gray bars, VLCAD$^{-/-}$; white bars, LCAD-/-.

DISCUSSION

Inborn errors of long-chain FAO represent unique diagnostic challenges. Ranges in disease phenotype can be significant not only among patients with different enzyme deficiencies, but among patients with the same disorder (3,7,10). Indeed, many patients present with metabolic profiles typical of inborn errors of FAO for whom a particular enzyme deficiency cannot be identified. These patients could represent a population with disease arising from a heterozygous dosage effect (17). In these cases, the effects of mutations in one allele in two or more functionally related genes combine to produce a disease phenotype that resembles the phenotypes seen in single gene deficiencies. We have called this condition synergistic heterozygosity (17). We have reported here mouse models that feature homozygous null mutations in two closely related metabolic genes with respect to metabolic function, LCAD and VLCAD.

The pattern of inborn fatty acid metabolic disease, similar to that seen in humans, occurs when mutant mice are challenged with fasting. Clearly, LCAD$^{-/-}$ mice show a more severe phenotype than VLCAD$^{-/-}$ mice. For example, both LCAD$^{-/-}$ and VLCAD$^{-/-}$ mice develop hepatosteatosis in response to fasting with the most severe fatty infiltration seen in LCAD$^{-/-}$ mice (Fig. 3). The presence of cardiac fibrosis in LCAD$^{-/-}$ mice has been reported (15), as has cold intolerance in LCAD$^{-/-}$ mice (18). Other investigators have described cold intolerance in VLCAD-deficient mice, as well as death in response to prolonged fasting and cold stress (19,20). The relative rise in abnormal metabolites associated with the different enzyme deficiencies is consistent with other phenotypic features as LCAD$^{-/-}$ mice accumulate more total long-chain acylcarnitine than VLCAD$^{-/-}$ mice. The normal fecundity of VLCAD$^{-/-}$ breeders compared with LCAD$^{-/-}$ breeders reiterates the theme of attenuated disease arising out of VLCAD deficiency when compared with LCAD deficiency.

We hypothesized that differences in the build-up of abnormal metabolites between LCAD- and VLCAD-deficient mice could contribute to greater disease severity in LCAD$^{-/-}$ mice. The cellular mechanisms for trafficking LCFAs, the intracellular fatty acid binding proteins, are structured to transport the C_{16} and C_{18} fatty acid overflow associated with VLCAD deficiency better than the C_{14} metabolite accumulation associated with LCAD deficiency. Even the liver fatty acid binding protein, the protein considered to have the broadest range of fatty acid substrates with high affinity binding, does not bind myristate (C_{14}) (21). This may allow for greater accumulations of C_{14} metabolites, slower export, and greater opportunity for toxic metabolites to interact with cell signaling mechanisms. Such alterations may be associated with the fasting. The disparity between the phenotype severity of VLCAD deficiency in mice and that seen in VLCAD-deficient patients may lie with interspecies differences in enzyme abundance or differences for substrate affinity, resulting in the relatively high reliance on VLCAD activity in humans. There are several indications of this. First, human patients with VLCAD mutations had low ability to oxidize palmitate in fibroblasts or dehydrogenate palmitoyl-CoA in fibroblast extracts (10,22). This indicated that there is little LCAD activity present in human fibroblasts; however, comparable liver data were not available on the same patients. In studies by others (13), human LCAD expression is not completely co-located with VLCAD expression, indicating that in humans LCAD may play a role in tissues where VLCAD is not expressed. In contrast, using cultured mouse fibroblasts we demonstrated that ~30–40% of palmitoyl-CoA dehydrogenation occurred via LCAD (15), indicating that mouse fibroblasts appear to rely more on LCAD for β-oxidation. Furthermore, in mouse fibroblasts no differences in palmitate oxidation were noted between the fibroblasts of VLCAD-deficient mice and wild-type controls (data not shown). Additionally, control human liver showed that 17% of palmitoyl-CoA dehydrogenation is due to LCAD, whereas 40% is due to LCAD in rats (23), and in the current study, the mouse value was ~25%. Data on LCAD activity in other human tissues have not been reported. We speculate that a protective functional redundancy in activity toward palmitate may be provided by LCAD activity in VLCAD$^{-/-}$ mice, as supported by the observation that LCAD$^{-/-}$//VLCAD$^{-/-}$ progeny fail to survive after birth. Another related explanation for the attenuated disease severity in VLCAD$^{-/-}$ mice compared with VLCAD-deficient patients may be a compensatory increase of LCAD activity in VLCAD-deficient mice. This possibility, however, was not supported by assays of enzyme activities in the mouse models. Activity toward 2,6-dimethylheptanoyl-CoA, apparently specific for LCAD activity (16) and absent in LCAD$^{-/-}$ mice, was not increased in VLCAD$^{-/-}$ mice (Table 1).

From a clinical standpoint, it is important to note that the correlation between *in vitro* enzyme activity and *in vivo* biological function is poor. Based on the robust activity of LCAD toward $C_{18:1}$ acyl-CoA *in vitro* (Table 1), one would predict that $C_{18:1}$ conjugated metabolites would accumulate to higher levels in LCAD$^{-/-}$ mice than VLCAD$^{-/-}$ mice, when just the opposite is the case. This could be explained by considering the functional characteristics of these enzymes *in vivo*

versus those found *in vitro*. We speculate that the microenvironment of the mitochondria may confer a different substrate specificity range from that seen in *in vitro* analysis. If the *in vitro* conditions chosen do not accurately reflect the maximal activity VLCAD toward $C_{18:1}$ acyl-CoA, it is possible that VLCAD indeed compensates for lost LCAD activity toward this substrate. In any case, the point can be made that metabolic outcomes of a given enzyme deficiency cannot always be predicted by enzyme activity *in vitro*.

Other clinical considerations demonstrated here were the reliability and sensitivity of abnormal metabolite detection in whole blood, bile, urine and serum, along with the specificity of LCAD toward the branched-chain fatty acid substrate 2,6-dimethylheptanoyl-CoA (16). Some have speculated that LCAD activity is directed mainly toward branched-chain fatty acid substrates (16). It is conceivable that disrupted branch-chain fatty acid catabolism forms the basis for greater disease severity in LCAD-deficient mice. While this may be possible in human beings, it appears unlikely in mice. Chromatographs of blood and bile acylcarnitine species failed to show detectable accumulations of such predicted metabolites, e.g. 2,6-dimethylheptanoyl-carnitine, where they would seem likely to occur were they the basis of the greater disease severity seen in $LCAD^{-/-}$ mice. Our collective data strongly indicated a deficiency in straight-chain fatty acid catabolism.

These mouse models for acyl-CoA dehydrogenase deficiencies displayed some of the physiologic and biochemical complexities that still baffle our understanding of inborn errors of metabolism, not to mention the diagnostic and therapeutic challenges these disorders pose. We anticipate that some answers and probably new challenges will originate from future investigations of the mechanisms that underlie the phenotypic complexities in these mouse models, leading to improved clinical management of children suffering from these potentially life-threatening disorders.

MATERIALS AND METHODS

Generation of VLCAD-deficient mouse model

The *Acadvl* targeting vector was constructed from genomic DNA fragments derived from a mouse 129/Ola genomic P1 clone, PV1. The P1 clone was identified by screening a mouse 129/Ola strain genomic library by PCR (Genome Systems, St Louis, MO). An ~17 kb *Xho*I fragment, PV XhoLMW-3, which included the promoter and the first six exons and a portion of intron 6, comprised the long arm. A 3.3 kb *Pst*I fragment designated PV *Pst*-4, including a portion of exon 20, the 3′ untranslated region of *Acadvl* and a portion of the mouse disheveled homolog gene (*Dvl2*), comprised the short arm. Care was taken to avoid disruption of the *Dvl2* gene that resides just 3′ to the *Acadvl* gene on chromosome 11 (24). The neomycin resistance gene (*neo*) under the control of the phosphoglycerate kinase promoter and a bovine poly(A) signal were derived from the pNTK vector (25) (Fig. 1). Linearized vector was electroporated into TC-1 embryonic stem cells derived from 129Sv/EvTacfBR (129) mice and G418-resistant clones were analyzed by Southern blot (15). Correctly targeted ES cell clones were microinjected into C57BL/6NTTacfBR (B6) blastocysts (Taconic, Germantown, NY) to generate chimeras that were then crossed to B6 mice. Subsequent generations were intercrosses among B6, 129 progeny.

Mice

All mice in the study were homozygous at either the *Acadl* locus (B6 129-$Acadl^{tm1Uab}$) ($LCAD^{-/-}$) or the *Acadvl* locus (B6 129-$Acadvl^{tm1Uab}$) ($VLCAD^{-/-}$), or had B6 129-$Acadl^{+/+}$ and B6 129-$Acadvl^{+/+}$ wild-type alleles (normal controls). An equivalent B6 129 background was maintained by using intercrosses within all three genotypes. Mice were negative for murine pathogens based on serological assays for 10 different viruses, aerobic bacterial cultures of nasopharynx and cecum, examinations for endo- and ectoparasites, and histopathology of all major organs. All animal protocols were approved by the Institutional Animal Care and Use Committee of the University of Alabama at Birmingham.

Sample collection

Prior to death and sample collection, all mice were fasted for ~24 h. Blood was collected from the retro-orbital venous plexus under surgical anesthesia using intraperitoneal administration of Avertin to effect. Whole blood samples were allowed to coagulate at room temperature followed by storage on ice until the sera were isolated. Organs used for tissue metabolite profile measurements or Oil-Red-O staining were snap frozen in liquid nitrogen and stored at –80°C until processed.

Mass spectrometry determination of tissue, serum and blood spot acylcarnitine profile

Acylcarnitines were measured in serum (26) and bile (27) by electrospray tandem mass spectrometry (ESI-MS/MS; Perkin Elmer Sciex API 2000). To each bile sample, six internal standards of known concentration and acetonitrile for deproteinization were added. Following agitation for 30 min and centrifugation, the supernatant was dried and then treated with n-butanol HCl, yielding the acylcarnitines as their n-butylesters for analysis by ESI-MS/MS. The concentrations of the analytes were established by computerized comparison of ion intensities of these analytes with that of the closest internal standard. Blood spot and snap frozen liver, heart and skeletal muscle tissues were analyzed for specific acylcarnitine derivatives by using fast-atom bombardment-tandem mass spectrometry (28).

Urinary dicarboxylic acid analysis

Urine samples were diluted to 1 ml, acidified and then extracted five times with 2 ml of ethyl acetate. After evaporation, the dry residue was silylated with 100 µl of *N*,*O*-bis(trimethylsilyl)trifluoroacetamide with 1% trimethylchlorosilane and analyzed by capillary gas chromatography/mass spectrometry (GC/MS) using the analytical conditions described previously (29). Quantitation of dicarboxylic acids was performed in ratio to the internal standard pentadecanoic acid using standard calibration curves at six concentration levels.

Serum and tissue fatty acid measurement

Serum and tissue FFAs (C_8–C_{26}) were measured using GC/MS as described previously (15,30).

Enzymology

Mitochondria were isolated from liver tissue of 6-week-old mice and western blot analysis was performed on 50 µg of mitochondrial protein as described using anti-VLCAD antibodies (31). Enzyme activities toward palmitoyl-CoA (C_{16}), octanoyl-CoA (C_8), oleoyl-CoA ($C_{18:1}$) and 2,6-dimethylheptanoyl-CoA (C_9) were assayed using extracts from frozen liver and heart muscle in the ETF fluorescence-reduction assay originally described by Frerman and Goodman (32) with further modifications by us (33). Results are expressed as mU/mg protein, where one unit equals 1 µmol ETF reduced/min.

Statistical analysis

Statistical analysis was performed using a univariate linear model and one-way analysis of variance (ANOVA) in the Sigma-Stat software package (SPSS Inc., Chicago, IL). χ^2 analysis was performed using standard methods.

ACKNOWLEDGEMENTS

We thank Philip Leder and Chuxia Ding for providing the TC-1 ES cells, Ronald J.A.Wanders for providing the 2,6 dimethylhepatanoyl-CoA and the UAB Transgenic Animal/ES Cell Resource (P30-CA13148). This work was supported by NIH grants RO1-RR02599 (P.A.W.) and RO1-DK45482 (J.V.) and training grant T-32-RR00493 (K.B.C.).

REFERENCES

1. Bennett, M.J., Rinaldo, P. and Strauss, A.W. (2000) Inborn errors of mitochondrial fatty acid oxidation. *Crit. Rev. Clin. Lab. Sci.*, **37**, 1–44.
2. Vianey-Saban, C., Divry, P., Brivet, M., Nada, M., Zabot, M.T., Mathieu, M. and Roe, C.R. (1998) Mitochondrial very-long-chain acyl-coenzyme A dehydrogenase deficiency: clinical characteristics and diagnostic considerations in 30 patients. *Clin. Chim. Acta*, **269**, 43–62.
3. Andresen, B.S., Olpin, S., Poorthuis, B.J., Scholte, H.R., Vianey-Saban, C., Wanders, R., Ijlst, L., Morris, A., Pourfarzam, M., Bartlett, K. *et al.* (1999) Clear correlation of genotype with disease phenotype in very-long-chain acyl-CoA dehydrogenase deficiency. *Am. J. Hum. Genet.*, **64**, 479–494.
4. Yamaguchi, S., Indo, Y., Coates, P.M., Hashimoto, T. and Tanaka, K. (1993) Identification of very-long-chain acyl-CoA dehydrogenase deficiency in three patients previously diagnosed with long-chain acyl-CoA dehydrogenase deficiency. *Pediatr. Res.*, **34**, 111–113.
5. Olpin, S.E., Bonham, J.R., Downing, M., Manning, N.J., Pollitt, R.J., Sharrard, M.J. and Tanner, M.S. (1997) Carnitine-acylcarnitine translocase deficiency – a mild phenotype. *J. Inherit. Metab. Dis.*, **20**, 714–715.
6. Pande, S.V. (1999) Carnitine-acylcarnitine translocase deficiency. *Am. J. Med. Sci.*, **318**, 22–27.
7. Bonnefont, J.P., Taroni, F., Cavadini, P., Cepanec, C., Brivet, M., Saudubray, J.M., Leroux, J.P. and Demaugre, F. (1996) Molecular analysis of carnitine palmitoyltransferase II deficiency with hepatocardiomuscular expression. *Am. J. Hum. Genet.*, **58**, 971–978.
8. Izai, K., Uchida, Y., Orii, T., Yamamoto, S. and Hashimoto, T. (1992) Novel fatty acid β-oxidation enzymes in rat liver mitochondria. Purification and properties of very-long-chain acyl-coenzyme A dehydrogenase. *J. Biol. Chem.*, **267**, 1027–1033.
9. Ikeda, Y., Okamura-Ikeda, K. and Tanaka, K. (1985) Purification and characterization of short-chain, medium-chain, and long-chain acyl-CoA dehydrogenases from rat liver mitochondria. Isolation of the holo- and apoenzymes and conversion of the apoenzyme to the holoenzyme. *J. Biol. Chem.*, **260**, 1311–1325.
10. Mathur, A., Sims, H.F., Gopalakrishnan, D., Gibson, B., Rinaldo, P., Vockley, J., Hug, G. and Strauss, A.W. (1999) Molecular heterogeneity in very-long-chain acyl-CoA dehydrogenase deficiency causing pediatric cardiomyopathy and sudden death. *Circulation*, **99**, 1337–1343.
11. Aoyama, T., Souri, M., Ueno, I., Kamijo, T., Yamaguchi, S., Rhead, W.J., Tanaka, K. and Hashimoto, T. (1995) Cloning of human very-long-chain acyl-coenzyme A dehydrogenase and molecular characterization of its deficiency in two patients. *Am. J. Hum. Genet.*, **57**, 273–283.
12. Strauss, A.W., Powell, C.K., Hale, D.E., Anderson, M.M., Ahuja, A., Brackett, J.C. and Sims, H.F. (1995) Molecular basis of human mitochondrial very-long-chain acyl-CoA dehydrogenase deficiency causing cardiomyopathy and sudden death in childhood. *Proc. Natl Acad. Sci. USA*, **92**, 10496–10500.
13. Andresen, B.S., Bross, P., Vianey-Saban, C., Divry, P., Zabot, M.T., Roe, C.R., Nada, M.A., Byskov, A., Kruse, T.A., Neve, S. *et al.* (1996) Cloning and characterization of human very-long-chain acyl-CoA dehydrogenase cDNA, chromosomal assignment of the gene and identification in four patients of nine different mutations within the VLCAD gene. *Hum. Mol. Genet.*, **4**, 461–472.
14. Souri, M., Aoyama, T., Orii, K., Yamaguchi, S. and Hashimoto, T. (1996) Mutation analysis of very-long-chain acyl-coenzyme A dehydrogenase (VLCAD) deficiency: identification and characterization of mutant VLCAD cDNAs from four patients. *Am. J. Hum. Genet.*, **8**, 97–106.
15. Kurtz, D.M., Rinaldo, P., Rhead, W.J., Tian, L., Millington, D.S., Vockley, J., Hamm, D.A., Brix, A.E., Lindsey, J.R., Pinkert, C.A. *et al.* (1998) Targeted disruption of mouse long-chain acyl-CoA dehydrogenase gene reveals crucial roles for fatty acid oxidation. *Proc. Natl Acad. Sci. USA*, **95**, 15592–15597.
16. Wanders, R.J.A., Denis, S., Ruiter, J., IJlst, L. and Dacremont, G. (1998) 2,6-Dimethylheptanoyl-CoA is a specific substrate for long-chain acyl-CoA dehydrogenase (LCAD): Evidence for a major role of LCAD in branch-chain fatty acid oxidation. *Biochim. Biophys. Acta*, **1393**, 35–40.
17. Vockley, J., Rinaldo, P., Bennett, M.J., Matern, D. and Vladutiu, G.D. (2000) Synergistic heterozygosity: disease resulting from multiple partial defects in one or more metabolic pathways. *Mol. Genet. Metab.*, **71**, 10–18.
18. Guerra, C., Koza, R.A., Walsh, K., Kurtz, D.M., Wood, P.A. and Kozak, L.P. (1998) Abnormal nonshivering thermogenesis in mice with inherited defects of fatty acid oxidation. *J. Clin. Invest.*, **102**, 1724–1731.
19. Exil, V.J., Sims, H., Qin, W., Boero, J., Khuchua, Z. and Strauss, A.W. (1999) Stress-induced death in the very-long-chain acyl-CoA dehydrogenase deficient mouse. *Circulation*, **100**, 2594–2595.
20. Exil, V.J., Sims, H., Kovacs, A., Qin, W., Boero, J., Khuchua, Z. and Strauss, A.W. (1998) Physiologic stressors inducing sudden death in the very-long-chain acyl-CoA dehydrogenase deficient mice. *Circulation*, **98**, 1–5.
21. Lowe, J.B., Saccettini, J.C., Laposata, M., McQuillan, J.J. and Gordon, J.I. (1987) Expression of rat intestinal fatty acid-binding protein in *Escherichia coli*. *J. Biol. Chem.*, **262**, 5931–5937.
22. Aoyama, T., Souri, M., Ushikubo, S., Kamijo, T., Yamaguchi, S., Kelley, R.I., Rhead, W.J., Uetake, K., Tanaka, K. and Hashimoto, T. (1995) Purification of human very-long-chain acyl-coenzyme A dehydrogenase and characterization of its deficiency in seven patients. *J. Clin. Invest.*, **95**, 2465–2473.
23. Lea, W., Abbas, A.S., Sprecher, H., Vockley, J. and Schulz, H. (2000) Long-chain acyl-CoA dehydrogenase is a key enzyme in the mitochondrial β-oxidation on unsaturated fatty acids. *Biochim. Biophys. Acta*, **1485**, 121–128.
24. Cox, K.B., Johnson, K.R. and Wood, P.A. (1998) Chromosomal locations of the mouse fatty acid oxidation genes Cpt1a, Cpt1b, Cpt2, Acadvl, and metabolically related Crat gene. *Mamm. Genome*, **9**, 608–610.
25. Ausubel, F.M., Brent, R., Kingston, R.E., Moore, D.D., Seidman, J.G., Smith, J.A. and Struhl, K. (1988) In Chandra, V.B. (ed.), *Current Protocols in Molecular Biology*, Vol. 1. Greene Publishing Associates, New York, pp. 9.16.1–9.16.11.
26. Van Hove, J.L.K., Kahler, S.G., Feezor, M.D., Ramakrishna, J.P., Hart, P., Treem, W.R., Shen, J.-J., Matern, D. and Millington, D.S. (2000) Acylcarnitines in plasma and blood spots of patients with long-chain 3-hydroxyacylcoenzyme A dehydrogenase deficiency. *J. Inherit. Metab. Dis.*, **23**, 571–582.
27. Rashed, M.S., Ozand, P.T., Bennett, M.J., Barnard, J.J., Govindaraju, D.R. and Rinaldo, P. (1995) Diagnosis of inborn errors of

metabolism in sudden death cases by acylcarnitine analysis of postmortem bile. *Clin. Chem.*, **41**, 1109–1114.
28. Millington, D.S., Norwood, D.L., Kodo, N., Roe, C.R. and Inoue, F. (1989) Application of fast atom bombardment with tandem mass spectrometry and liquid chomatography/mass spectrometry to the analysis of acylcarnitines in human urine, blood, and tissue. *Anal. Biochem.*, **180**, 331–339.
29. Rinaldo, P., Welch, R.D, Previs, S.F., Schmidt-Sommerfeld, E., Gargus, J.J., O'Shea, J.J. and Zinn, A.B. (1991) Ethylmalonic/adipic aciduria: effect of oral medium chain triglycerides, carnitine and glycine on urinary excretion of organic acids, acylcarnitines and acylglycines. *Pediatr. Res.*, **30**, 216–221.
30. Boles, R.G., Martin, S.K., Blitzer, M.G. and Rinaldo, P. (1994) Biochemical diagnosis of fatty acid oxidation disorders by metabolite analysis of post-mortem liver. *Hum. Pathol.*, **25**, 733–734.
31. Amendt, B.A., Freneaux, E., Reece, C., Wood, P.A. and Rhead, W.J. (1992) Short-chain acyl-coenzyme A dehydrogenase activity, antigen, and biosynthesis are absent in the BALB/cByJ mouse. *Pediatr. Res.*, **31**, 552–556.
32. Frerman, F. and Goodman, S.I. (1985) Fluorometric assay of acyl-CoA dehydrogenases in normal and mutant human fibroblasts. *Biochem. Med.*, **33**, 38–44.
33. Vockley, J., Mohsen, A.W., Binzak, B., Willard, J. and Fauq, A. (2000) Mammalian branch-chain acyl-CoA dehydrogenases: molecular cloning and characterization on the recombinant enzymes. *Methods Enzymol.*, **324**, 241–258.